Influence of the Arctic Sea-Ice Regime Shift on Sea-Ice Methylated Mercury Trends

Amina Schartup, Anne Soerensen, Lars-Eric Heimbürger-Boavida

Influence of Arctic Sea-Ice Regime Shift on Sea-Ice Methylated Mercury Trends

Amina T. Schartup,[1] Anne L. Soerensen[2] and Lars-Eric Heimbürger-Boavida[3]

[1]Scripps Institution of Oceanography, La Jolla CA, USA

[2]Swedish Museum of Natural History, Department of Environmental Research and Monitoring, Stockholm, Sweden

[3]Aix Marseille Université, CNRS/INSU, Mediterranean Institute of Oceanography (MIO) UM 110, Marseille, France

Correspondence to: aschartup@ucsd.edu

Abstract

Arctic sea-ice regulates the air-sea exchange of volatile mercury (Hg) species like dimethylmercury (DMHg) or elemental Hg, and is known to host Hg methylating microbes that produce neurotoxic and biomagnifying monomethylmercury (MMHg). Arctic sea-ice accounts for 57% of the total primary production in the Arctic Ocean suggesting that it could be the main source of MMHg to arctic food-webs. Despite this, little is known about Hg concentrations and speciation in arctic sea-ice. Here, we report Hg species and show the importance of sea ice composition on sea-ice methylmercury (MeHg = DMHg+MMHg) budgets. We propose that the shift from older sea-ice (lower MeHg) to younger sea-ice (higher MeHg) resulted in a 40% increase in MeHg (per m^2 of sea-ice) since 1979 despite a 45% decline in the total sea-ice

volume. About 30% of the MeHg sea-ice budget is DMHg, this means that when the sea-ice melts in the summer it could contribute 0.03 - 2.7 pmol m^{-2} day^{-1} of DMHg to the atmosphere which is comparable to diffusion from water (0.48 - 2.8 pmol m^{-2} day^{-1}). This study shows that the MeHg content of rapidly shrinking arctic sea-ice and exposure of sea-ice biota may not be declining as previously thought.

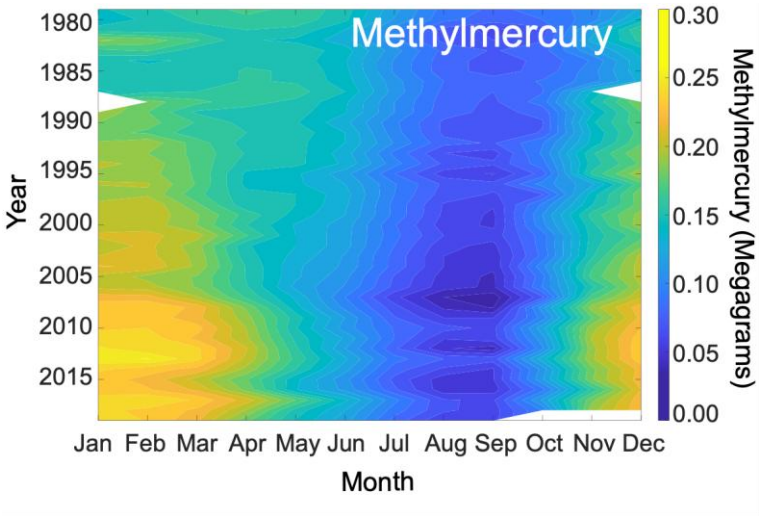

TOC abstract

Keywords: Dimethylmercury, monomethylmercury, climate change, GEOTRACES

Introduction

The Arctic Ocean's unique physical characteristics and food-web structure influence the biogeochemical cycle of neurotoxic monomethylmercury (MMHg), allowing it to reach high levels in arctic biota.[1,2] In the Arctic, MMHg is a health concern for marine wildlife and human communities dependent on arctic ecosystems for hunting and fishing.[1,3] Among the physical characteristics, the presence of sea-ice has been identified as a possible explanation for the higher production and biomagnification of MMHg observed in the Arctic Ocean.[2] Sea-ice regulates air-sea exchange of volatile Hg species (elemental Hg-Hg^0 and dimethylmercury - DMHg) by capping the water column and letting Hg build up under the ice.[4,5] The mechanism of sea-ice production and melting creates a highly stratified surface water column that has been proposed to enhance MMHg production.[6–8] Sea-ice can also impact MMHg exposure through biologically mediated MeHg production within the sea-ice itself, as suggested by Beattie *et al.*[9] based on a study of total methylated Hg species (MeHg = MMHg + DMHg) in two arctic sea-ice cores. Several studies showed a positive correlation between chlorophyll a (a proxy for primary production) and MeHg concentration in arctic and antarctic sea-ice, suggesting that MeHg is biologically produced.[9–11] Recently, Gionfriddo *et al.*[11] further identified putative Hg methylating bacteria (*Nitrospina*) in antarctic first-year ice (FYI) and arctic frost flowers, but the mechanism of Hg methylation in sea ice remains unknown. Compared to other arctic MMHg reservoirs the total amount of MMHg stored in sea-ice is small,[12] but arctic sea-ice algae and sub-ice phytoplankton account for 57% of the total annual primary production in the Arctic Ocean.[13,14] This implies that MMHg produced in the sea-ice and bioaccumulated by sea-ice algae, may contribute disproportionally to arctic biota MMHg exposure. Since 1958, the average

sea-ice thickness has declined by over 60% (more than 2 m).[15] Between 2002 and 2017, the Arctic has lost more than 50% of its oldest multi-year ice (MYI),[15] and is undergoing a regime shift from a system dominated by MYI (until 2011) to a system dominated by seasonal ice (FYI). Despite these concerns, relatively few studies have reported concentrations of Hg and MeHg in sea-ice.[5,9,16]. To address this gap, we collected 6 ice cores (2 MYI and 4 FYI), brine, frost flowers, under-ice water, and melt pond water and ice during the 2015 German GEOTRACES expedition (GN04). We measured total Hg and MeHg in all the samples and MMHg and DMHg in 3 of the cores. To extend the spatial coverage of this study we combine our data with sea-ice total Hg and MeHg samples from 5 additional locations collected in 2015 during the U.S. GEOTRACES expedition (GN01).[5]

Methods

Six cores were collected between Aug 25 and Sept 22 during the 2015 GEOTRACES expedition (Figure 1A, Figure S1). At each site, a Kovacs 9 cm diameter corer (Kovacs Enterprise, Roseburg, USA) was used. Once retrieved, the cores were sectioned into 10 cm slices, cleaned with a ceramic knife and transferred into clean plastic bags. The slices were thawed and transferred into trace metal clean bottles (Nalgene FEP Teflon) while still very cold to minimize loss of volatile Hg. All samples were acidified to 0.4 % v:v with double-distilled hydrochloric acid. Temperature and salinity of each slice were measured during and shortly after collection, respectively (Figure S2). Two of the 6 cores were identified as MYI (Cores 2 and 5) on site.[17] We also measured total Hg and MeHg in 1 brine, 1 frost flower, 7 under ice seawater, 5 melt pond water, 2 melt pond ice, and 3 snow samples (Table S2). All samples were shipped and analyzed for total Hg and MeHg at Harvard University in May 2016 (Figure S3 and S4). We

followed well-established analytical procedures for low level total Hg and MeHg measurements.[18–20] Detailed methods and nutrient profiles are provided in the Supporting Information (Figure S5). MMHg was measured on samples from which DMHg had been removed by purging onboard prior to acidification. DMHg was calculated as the difference between MeHg and MMHg,[21,22] and inorganic Hg (Hg^{II}) as the difference between total Hg and MeHg (Figure S3). Table 1 summarizes the Hg speciation and ancillary data in the collected sea-ice cores. We calculated the brine volume according to Cox & Weeks.[23]

To estimate the impact of the shift from MYI dominated to FYI dominated sea-ice on MeHg, we obtained monthly sea-ice volumes and total sea area trends from 1979 to 2019 from the U.S. National Snow and Ice Data Center.[24] We use this information and the empirical relationship between sea-ice volume and MYI area reported by Kwok[15] to estimate respective contributions of FYI and MYI to the sea-ice volume and to the sea-ice MeHg budgets from 1979 to 2019. Total Hg concentrations measured in sea-ice cores in this study, 2.72 ± 2.31 pM (n = 78), are not statistically different (1-way ANOVA, p = 0.92, n = 126) from concentrations reported by DiMento *et al.*,[5] 2.54 ± 1.46 pM (n = 44; Figure S6). To increase the spatial coverage of this study, we include the DiMento *et al.*[5] sea-ice data in subsequent calculations. For continuity, we rename their cores 7-11 (Figure 1A). The cores in DiMento *et al.*[5] were not identified as FYI or MYI (Table S1), thus we rely on the sea-ice thickness reported for the coring sites in Marsay *et al.*[16] and the relationship between sea-ice thickness and age[25] to differentiate the cores (FYI: Core 7, 9; MYI: Cores 8, 10 and 11). All statistical analyses are done in MATLAB (Mathworks, version R2019b).

Results and Discussion

Total Hg varies within cores, with concentrations typically higher near the surface that decline sharply with core depth (Figure 1B; Figure S3). For example, in Core 4, concentrations span from 0.96 to 16.1 pM. Total Hg concentrations in brine, melt ponds water and ice, under ice water and snow fall within the ranges measured in the sea-ice cores and range from 2.6 pM in snow to 17.3 pM in brine (SI Table S2). There is no statistical difference (1-way ANOVA, $p = 0.34$, $n = 110$) between total Hg concentrations in FYI (3.00 ± 2.56 pM, $n = 57$) and MYI cores (2.57 ± 2.16 pM, $n = 53$).

Similar to total Hg, MeHg varies within each core (Figure S4). For example, MeHg concentrations in Core 3 range from 0.024 to 0.293 pM (Figure 1C). But the location of peaks is not always at the surface, MeHg peaks are also seen at depth in FYI cores (Core 4, Figure 1C). MeHg levels in brine, melt ponds water and ice, under ice water and snow also fall within ranges measured in the sea-ice cores, from 0.05 pM in snow to 0.19 pM in brine (Table S2). MeHg concentrations in MYI (0.026 ± 0.018 pM, $n = 52$) cores are lower (1-way ANOVA, $p < 0.01$, $n = 109$) than in FYI cores (0.102 ± 0.071 pM, $n = 57$). Since the total Hg (and Hg^{II}) concentrations in FYI and MYI cores are not significantly different, %MeHg is lower in MYI than FYI cores. Since Hg^{II} concentrations are similar in both types of cores, the difference in MeHg is probably not due to Hg^{II} limitation, but may instead be due to biological or chemical differences between the two types of sea-ice cores that affect *in situ* production or degradation of MeHg from Hg^{II}.[11,26,27]

Methylmercury peaks in FYI Cores 3 and 4 seem to be dictated by peaks in DMHg rather than MMHg (Figure 1C). On average DMHg is 34% of MeHg in the 3 cores where DMHg and MMHg were determined, but peaks at >90% at 120 cm in Core 4 (Figure 1C). The distribution of DMHg within cores is consistent with physically driven processes of bubble nucleation and migration observed for inert gases such as argon in FYI.[11,28] Since very little field data exists on trace gas bubble formation and diffusion through the sea-ice, modeling approaches have been used to test different hypotheses. Moreau *et al*.[29] showed that upward moving argon gas bubbles explain the change in argon profiles from a bottom peak found in "Early Spring" to a surface peak found in "Late Spring". They explain the migration by the melting of the sea-ice allowing brine channels to form (increasing the brine volume) and bubbles to rise. This is consistent with our data where Core 3 has a lower brine volume (4.3%) than Core 4 (5.1%, Figure S7). Core 3's DMHg profile aligns well with the "Early Spring" scenario while DMHg in Core 4 follows the "Late Spring" scenario in Moreau *et al*,[29] indicating that DMHg is at different stages of evasion.

We compare potential DMHg release from sea-ice to air with its diffusion from water column to air. Assuming that DMHg behaves similarly to argon, as described by Moreau *et al*.,[29] it builds up in the sea-ice during the winter months (January through May/June) and is released to the atmosphere in the spring when sea-ice starts melting.[30] We calculate that approximately 75 km^3 day^{-1} of FYI are lost due to sea-ice melt between peak and low volume in 2015 (120 days). If DMHg concentrations are uniform across all the cores (0.030 pM on average, ranging from 0.003 – 0.32 pM), 2.3 mol day^{-1} of DMHg (0.23- 24 mol day^{-1}) are released from the sea-ice during the melt season. Thus, melting sea-ice could release 0.25 pmol m^{-2} day^{-1} of DMHg over the sea-ice area in 2015 to the marine boundary layer (ranging from 0.03 - 2.7 pmol m^{-2} day^{-1}).

159 This is a conservative estimate since sea-ice only needs to reach a threshold porosity level (5-
160 7%), not completely melt, to start releasing DMHg, and some DMHg may have already been lost
161 prior to our sampling.[29] To compare the sea-ice DMHg release to diffusion from the water
162 column, we calculate diffusion using a surface water DMHg (1 m; 2015 U.S. GEOTRACES)
163 concentrations from Agather *et al*.[31] most of which were below their detection limit of 0.012 pM,
164 atmospheric DMHg concentrations measured by Baya *et al*.[4] for 30% ice cover (0.037 pmol m^{-3}),
165 and wind speed from Lesins *et al*.[32] (3 m s^{-1} at 10.4 m). We obtain a diffusion rate from the water
166 column ranging from 0.48 to 2.8 pmol m^{-2} day^{-1} depending on the relationship between gas
167 exchange and wind speed used.[33–35] This flux is in the same range as our conservative estimate
168 on DMHg degassing from melting sea-ice, which suggests two major impacts on the Arctic
169 Ocean Hg cycle. 1) It shows that sea-ice is an important source of DMHg to the arctic
170 atmosphere, and 2) that the early spring release of DMHg to the atmosphere from melting sea-ice
171 could reduce the concentration gradient between water and air thereby dampening the DMHg
172 diffusion from the water column.
173
174 MeHg levels in FYI cores (0.102 ± 0.071 pM, n = 57) are about 4 times greater than in MYI
175 cores (0.026 ± 0.018 pM, n = 52). Therefore, we hypothesize that all things kept equal a shift
176 from MYI to FYI could significantly impact the sea-ice MeHg budget and average
177 concentrations which could lead to higher sea-ice biota exposure.[1,36] To test this, we calculate the
178 temporal variability of the MeHg budget considering the impact of the shifts in FYI and MYI.
179 The purpose of this calculation is to evaluate whether the magnitude of the shift alone, while all
180 other parameters are kept constant, could result in a different overall trend in the sea-ice MeHg
181 budget. We do not consider other potential changes that may dampen or exacerbate MeHg

concentrations in sea-ice, nor do we attempt to simulate past MeHg concentrations. Figure 2 A and B illustrate the importance of considering MeHg concentrations in different sea-ice types. In Figure 2A, we applied the average MeHg concentration to the total volume of sea-ice. We find that the average sea-ice budget over the 41-year period is 0.33 Mg (ranging from 0.04 Mg for minimum MeHg and sea-ice volume year, to 1.0 Mg for maximum MeHg and sea-ice volume year). This is consistent with previously reported reservoir sizes of 0.3-2.6 Mg that were based on two sea-ice cores collected in the Beaufort Sea and M'Clure Strait.[9,12] This approach results in a MeHg decline of 5.2 kg $year^{-1}$ mirroring the overall decline in sea-ice volume. However, if we instead account for the regime shift from MYI to FYI and the different MeHg concentrations in two ice types over the same time period, we arrive at a sea-ice reservoir of 0.16 Mg (ranging from 0.07 to 0.31 Mg). But more importantly, we do not see a declining MeHg trend despite the 45% sea-ice volume decline, instead we see a slight increase in MeHg of 1.3 kg $year^{-1}$. The September trend (minimum sea-ice cover; bottom of the shaded blue area in Figure 2B) is declining 0.5 kg $year^{-1}$ because of the large decline in total sea-ice volume. The high bound in February (maximum sea-ice cover) is increasing 3.3 kg $year^{-1}$ driven by the FYI increase over time. The change in the MeHg mass budget corresponds to an increase in mass of MeHg per area of sea-ice from 15 ng m^{-2} in the 1980s to 21 ng m^{-2} in the 2010s (orange line on Figure 2B). This suggests a 40% increase in the exposure of sea-ice biota and underlines the importance of understanding MeHg biogeochemistry in different types of sea-ice.

This study shows that sea-ice plays a role in Hg biogeochemistry that extends beyond "just a cap" on water column processes. We find that FYI contains more MeHg (and DMHg) than MYI and calculate that the ongoing shift from a MYI to FYI dominated Arctic Ocean may cancel out

the previously expected decline in MeHg contributions from sea-ice. This finding as well as the shortened window between sea-ice melt and peak plankton activity,[37,38] may have consequences for the exposure of biota that relies on sea-ice for food and habitat. We also measured relatively large amounts of DMHg in FYI cores, sometimes reaching >90% of MeHg. A DMHg peak was for example found near the bottom of a core where sea-ice algae such as *Melosira arctica* was present. DMHg could passively diffuse through gills of animals feeding on sea-ice algae[39] and the implications of DMHg in sea-ice highlighted in this study needs further investigation.

Acknowledgements:

We thank the chief scientist Ursula Schauer, the German GEOTRACES lead scientist Michiel Rutgers van der Loeff, and the sea-ice sampling team Gerhard Dieckmann, Ellen Damm, Christiane Uhlig, Aridane Gonzales Gonzales and Andreas Krell. We also thank Captain Schwarze and the crew of the research icebreaker Polarstern. ATS thanks Elsie Sunderland for years of support and exceptional mentorship and for access to her analytical lab at the Harvard School of Engineering and Applied Science where the reported mercury measurements were performed. ATS thanks Prentiss Balcom for assistance in the lab. LEHB thanks Jeroen Sonke from Geosciences Environment Toulouse for his support and guidance during his postdoc and partial support from the European Research Council (ERC-2010-StG_20091028) to Jeroen Sonke. LEHB also received support from AXA Research Fund and the CNRS Chantier Arctique Français funding via the Pollution in the Arctic System project.

Figure 1: Mercury concentrations and speciation in arctic sea-ice. Panel (A) is a map showing

the location of sea-ice cores in dark blue (1-6) collected for this study during the 2015 German GEOTRACES cruise, GN04 carried out on board of the research icebreaker Polarstern (PS94, ARK XXIX/3, TransArc-II), and in light blue (7-11) published in DiMento *et al*.[5] and collected during the 2015 U.S. GEOTRACES expedition (GN01). The sea-ice extent is an August 16th, 2015 Multisensor Analyzed Sea Ice Extent data product, US National Snow and Ice Data Center. Panel (B) shows total mercury (total Hg) profiles of Cores 3 and 4. Panel (C) shows monomethylmercury (MMHg), dimethylmercury (DMHg) and total methylated mercury (MeHg) distribution in Cores 3 and 4.

Figure 2: Sea-ice methylmercury (MeHg) budgets calculated from 1979 to 2019. **A.** Trend when differences in MeHg levels in multi-year and first-year ice are not considered. The shaded area captures the lowest (September) and highest (February) bounds of the sea ice MeHg budgets. **B.** The MeHg total mass budget, considering different contributions from multi-year and first-year sea-ice, is illustrated by the blue line. The blue shaded area captures the lowest (September) and highest (February) bounds of the sea-ice MeHg budgets. The MeHg mass per unit of sea-ice area is the orange line.

References

(1) AMAP. *Arctic Monitoring and Assessment Program 2011: Mercury in the Arctic*; 2011. https://doi.org/10.1017/CBO9781107415324.004.

(2) Zhang, Y.; Soerensen, A. L.; Schartup, A. T.; Sunderland, E. M. A Global Model for Methylmercury Formation and Uptake at the Base of Marine Food Webs. *Global Biogeochem. Cycles* **2020**, *34* (2). https://doi.org/10.1029/2019GB006348.

(3) Calder, R. S. D.; Bromage, S.; Sunderland, E. M. Risk Tradeoffs Associated with Traditional Food Advisories for Labrador Inuit. *Environ. Res.* **2019**, No. September, 496–506. https://doi.org/10.1016/j.envres.2018.09.005.

(4) Baya, P. A.; Gosselin, M.; Lehnherr, I.; Louis, V. L. S.; Hintelmann, H. Determination of Monomethylmercury and Dimethylmercury in the Arctic Marine Boundary Layer. **2015**, 1–19.

(5) DiMento, B. P.; Mason, R. P.; Brooks, S.; Moore, C. The Impact of Sea Ice on the Air-Sea Exchange of Mercury in the Arctic Ocean. *Deep. Res. Part I Oceanogr. Res. Pap.* **2019**, *144* (October 2018), 28–38. https://doi.org/10.1016/j.dsr.2018.12.001.

(6) Wang, F.; Macdonald, R. W.; Armstrong, D. a; Stern, G. a. Total and Methylated Mercury in the Beaufort Sea: The Role of Local and Recent Organic Remineralization. *Environ. Sci. Technol.* **2012**, *46* (21), 11821–11828. https://doi.org/10.1021/es302882d.

(7) Heimbürger, L.; Sonke, J. E.; Cossa, D.; Point, D.; Lagane, C.; Laffont, L.; Galfond, B. T.; Nicolaus, M.; Rabe, B.; van der Loeff, M. R.; et al. Shallow Methylmercury Production in the Marginal Sea Ice Zone of the Central Arctic Ocean. *Sci. Rep.* **2015**, *5*, 10318. https://doi.org/10.1038/srep10318.

(8) Schartup, A. T.; Balcom, P. H.; Soerensen, A. L.; Gosnell, K. J.; Calder, R. S. D.; Mason,

R. P.; Sunderland, E. M. Freshwater Discharges Drive High Levels of Methylmercury in Arctic Marine Biota. *Proc. Natl. Acad. Sci.* **2015**, *112* (38), 11789–11794. https://doi.org/10.1073/pnas.1505541112.

(9) Beattie, S. A.; Armstrong, D.; Chaulk, A.; Comte, J.; Gosselin, M.; Wang, F. Total and Methylated Mercury in Arctic Multiyear Sea Ice. *Environ. Sci. Technol.* **2014**, *48* (10), 5575–5582. https://doi.org/10.1021/es5008033.

(10) Cossa, D.; Heimbürger, L.-E.; Lannuzel, D.; Rintoul, S. R.; Butler, E. C. V.; Bowie, A. R.; Averty, B.; Watson, R. J.; Remenyi, T. Mercury in the Southern Ocean. *Geochim. Cosmochim. Acta* **2011**, *75* (14), 4037–4052. https://doi.org/10.1016/j.gca.2011.05.001.

(11) Gionfriddo, C. M.; Tate, M. T.; Wick, R. R.; Schultz, M. B.; Zemla, A.; Thelen, M. P.; Schofield, R.; Krabbenhoft, D. P.; Holt, K. E.; Moreau, J. W.; et al. Microbial Mercury Methylation in Antarctic Sea Ice. *Nat. Microbiol.* **2016**, *1* (August), 16127. https://doi.org/10.1038/nmicrobiol.2016.127.

(12) Soerensen, A. L.; Jacob, D. J.; Schartup, A. T.; Fisher, J. A.; Lehnherr, I.; St Louis, V. L.; Heimbürger, L. E.; Sonke, J. E.; Krabbenhoft, D. P.; Sunderland, E. M. A Mass Budget for Mercury and Methylmercury in the Arctic Ocean. *Global Biogeochem. Cycles* **2016**, *30* (4), 560–575. https://doi.org/10.1002/2015GB005280.

(13) Gosselin, M.; Levasseur, M.; Wheeler, P. A.; Horner, R. A.; Booth, B. C. New Measurements of Phytoplankton and Ice Algal Production in the Arctic Ocean. *Deep. Res. Part II Top. Stud. Oceanogr.* **1997**, *44* (8), 1623–1644. https://doi.org/10.1016/S0967-0645(97)00054-4.

(14) Boetius, A.; Albrecht, S.; Bakker, K.; Bienhold, C.; Felden, J.; Fernández-Méndez, M.; Hendricks, S.; Katlein, C.; Lalande, C.; Krumpen, T.; et al. Export of Algal Biomass from

the Melting Arctic Sea Ice. *Science (80-.).* **2013**, *339* (6126), 1430–1432. https://doi.org/10.1126/science.1231346.

(15) Kwok, R. Arctic Sea Ice Thickness, Volume, and Multiyear Ice Coverage: Losses and Coupled Variability (1958-2018). *Environ. Res. Lett.* **2018**, *13* (10). https://doi.org/10.1088/1748-9326/aae3ec.

(16) Chaulk, A.; Stern, G. A.; Armstrong, D.; Barber, D. G.; Wang, F. Mercury Distribution and Transport across the Ocean- Sea-Ice- Atmosphere Interface in the Arctic Ocean. *Environ. Sci. Technol.* **2011**, *45* (5), 1866–1872.

(17) Peeken, I.; Primpke, S.; Beyer, B.; Gütermann, J.; Katlein, C.; Krumpen, T.; Bergmann, M.; Hehemann, L.; Gerdts, G. Arctic Sea Ice Is an Important Temporal Sink and Means of Transport for Microplastic. *Nat. Commun.* **2018**, *9* (1). https://doi.org/10.1038/s41467-018-03825-5.

(18) Munson, K. M.; Babi, D.; Lamborg, C. H. Determination of Monomethylmercury from Seawater with Ascorbic Acid-Assisted Direct Ethylation. *Limnol. Oceanogr. Methods* **2014**, *12* (1 JAN), 1–9. https://doi.org/10.4319/lom.2014.12.1.

(19) United States Environmental Protection Agency. *Method 1631, Revision E: Mercury in Water by Oxidation, Purge and Trap, and Cold Vapour Atomic Fluorescence Spectrometry*; Washington, DC, 2002.

(20) United States Environmental Protection Agency. *Method 1630: Methylmercury in Water by Distillation , Aqueous Ethylation , Purge and Trap, and Cold Vapor Atomic Fluorescence*; Washington, DC, 2001.

(21) Cossa, D.; Durrieu de Madron, X.; Schäfer, J.; Lanceleur, L.; Guédron, S.; Buscail, R.; Thomas, B.; Castelle, S.; Naudin, J.-J. The Open Sea as the Main Source of

Methylmercury in the Water Column of the Gulf of Lions (Northwestern Mediterranean Margin). *Geochim. Cosmochim. Acta* **2017**, *199*, 222–237. https://doi.org/10.1016/j.gca.2016.11.037.

(22) Rosati, G.; Heimbürger, L. E.; Melaku Canu, D.; Lagane, C.; Laffont, L.; Rijkenberg, M. J. A.; Gerringa, L. J. A.; Solidoro, C.; Gencarelli, C. N.; Hedgecock, I. M.; et al. Mercury in the Black Sea: New Insights From Measurements and Numerical Modeling. *Global Biogeochem. Cycles* **2018**, *32* (4), 529–550. https://doi.org/10.1002/2017GB005700.

(23) Cox, G. F. N.; Weeks, W. F. Equations for Determining the Gas and Brine Volumes in Sea Ice Samples. *CRREL Rep. (US Army Cold Reg. Res. Eng. Lab.* **1982**, *29* (102), 306–316. https://doi.org/10.3189/s0022143000008364.

(24) Fetterer, F., K. Knowles, W. N. Meier, M. Savoie, and A. K. W. Sea Ice Index, Version 3. NSIDC: National Snow and Ice Data Center. https://doi.org/10.7265/N5K072F8.

(25) Tschudi, M. A.; Stroeve, J. C.; Stewart, J. S. Relating the Age of Arctic Sea Ice to Its Thickness, as Measured during Nasa's ICESat and IceBridge Campaigns. *Remote Sens.* **2016**, *8* (6). https://doi.org/10.3390/rs8060457.

(26) Bowman, J. S.; Rasmussen, S.; Blom, N.; Deming, J. W.; Rysgaard, S.; Sicheritz-Ponten, T. Microbial Community Structure of Arctic Multiyear Sea Ice and Surface Seawater by 454 Sequencing of the 16S RNA Gene. *ISME J.* **2012**, *6* (1), 11–20. https://doi.org/10.1038/ismej.2011.76.

(27) Bowman, J. S. The Relationship between Sea Ice Bacterial Community Structure and Biogeochemistry: A Synthesis of Current Knowledge and Known Unknowns. *Elementa* **2015**, *3*, 1–20. https://doi.org/10.12952/journal.elementa.000072.

(28) Zhou, J.; Delille, B.; Eicken, H.; Vancoppenolle, M.; Brabant, F.; Carnat, G.; Geilfus, N.

X.; Papakyriakou, T.; Heinesch, B.; Tison, J. L. Physical and Biogeochemical Properties in Landfast Sea Ice (Barrow, Alaska): Insights on Brine and Gas Dynamics across Seasons. *J. Geophys. Res. Ocean.* **2013**, *118* (6), 3172–3189. https://doi.org/10.1002/jgrc.20232.

(29) Moreau, S.; Vancoppenolle, M.; Zhou, J.; Tison, J. L.; Delille, B.; Goosse, H. Modelling Argon Dynamics in First-Year Sea Ice. *Ocean Model.* **2014**, *73*, 1–18. https://doi.org/10.1016/j.ocemod.2013.10.004.

(30) Miller, L. A.; Papakyriakou, T. N.; Collins, R. E.; Deming, J. W.; Ehn, J. K.; MacDonald, R. W.; Mucci, A.; Owens, O.; Raudsepp, M.; Sutherland, N. Carbon Dynamics in Sea Ice: A Winter Flux Time Series. *J. Geophys. Res. Ocean.* **2011**, *116* (2), 6058. https://doi.org/10.1029/2009JC006058.

(31) Agather, A. M.; Hammerschmidt, C. R.; Lamborg, C. H.; Bowman, K. L. Distribution of Mercury Species in the Western Arctic Ocean (U.S. GEOTRACES GN01). **2016**, No. May. https://doi.org/10.1130/abs/2016nc-275172.

(32) Lesins, G.; Duck, T.; Drummond, J. Climate Trends at Eureka in the Canadian High Arctic. *Atmos. - Ocean* **2010**, *48* (2), 59–80. https://doi.org/10.3137/AO1103.2010.

(33) Wanninkhof, R. Relationship between Wind Speed and Gas Exchange over the Ocean Revisited. *J. Geophys. Res.* **1992**, *97* (C5), 7373–7382. https://doi.org/10.4319/lom.2014.12.351.

(34) Liss, P. S.; Merlivat, L. Air-Sea Gas Exchange Rates: Introduction and Synthesis. In *The Role of Air-Sea Exchange in Geochemical Cycling*; Springer Netherlands: Dordrecht, 1986; pp 113–127. https://doi.org/10.1007/978-94-009-4738-2_5.

(35) Nightingale, P. D.; Malin, G.; Law, C. S.; Watson, A. J.; Liss, P. S.; Liddicoat, M. I.;

Boutin, J.; Upstill-Goddard, R. C. In Situ Evaluation of Air-Sea Gas Exchange Parameterizations Using Novel Conservative and Volatile Tracers. *Global Biogeochem. Cycles* **2000**, *14* (1), 373–387. https://doi.org/10.1029/1999GB900091.

(36) Schartup, A. T.; Qureshi, A.; Dassuncao, C.; Thackray, C. P.; Harding, G.; Sunderland, E. M. A Model for Methylmercury Uptake and Trophic Transfer by Marine Plankton. *Environ. Sci. Technol.* **2018**, *52* (2), 654–662. https://doi.org/10.1021/acs.est.7b03821.

(37) Post, E.; Bhatt, U. S.; Bitz, C. M.; Brodie, J. F.; Fulton, T. L.; Hebblewhite, M.; Kerby, J.; Kutz, S. J.; Stirling, I.; Walker, D. A. Ecological Consequences of Sea-Ice Decline. *Science (80-.).* **2013**, *341* (August), 519–525. https://doi.org/10.1126/science.1235225.

(38) Wassmann, P. Arctic Marine Ecosystems in an Era of Rapid Climate Change. *Prog. Oceanogr.* **2011**, *90* (1–4), 1–17. https://doi.org/10.1016/j.pocean.2011.02.002.

(39) Cossa, D.; Martin, J. M.; Sanjuan, J.; Martint, J.; Sanjuan, J. Dimethylmercury Formation in the Alboran Sea. *Mar. Pollut. Bull.* **1994**, *28* (6), 381–384. https://doi.org/10.1016/0025-326X(94)90276-3.

Table 1: Summary of sea-ice core characteristics and mean speciated mercury (Hg) concentrations (the standard deviation represents downcore variability).

Sea-ice Core	Station	Core thickness	Sea-ice Temperature	Salinity	Total Hg[†]	MeHg[‡]	DMHg[‡]	MeHg: Total Hg	DMHg: MeHg
		cm	°C		pM	pM	pM	%	%
1	46	85	-1.07	1.31	2.7±3.2	0.120±0.028	--	8.2	--
2	54*	167	-1.57	2.38	2.6±3.1	0.016±0.015	--	1.1	--
3	69	133	-1.73	1.37	3.0±1.9	0.086±0.101	0.048±0.094	3.0	34
4	81	135	-3.40	2.79	3.6±4.6	0.085±0.076	0.027±0.032	2.3	26
5	96*	151	-1.90	3.02	2.6±1.9	0.032±0.017	0.015±0.015	1.0	41
6	101	135	-4.08	3.45	2.5±0.8	0.115±0.043	--	5.0	--

* Multi-year sea-ice cores

[†] The method detection limit is 0.08 pM

[‡] The method detection limit is 0.011 pM

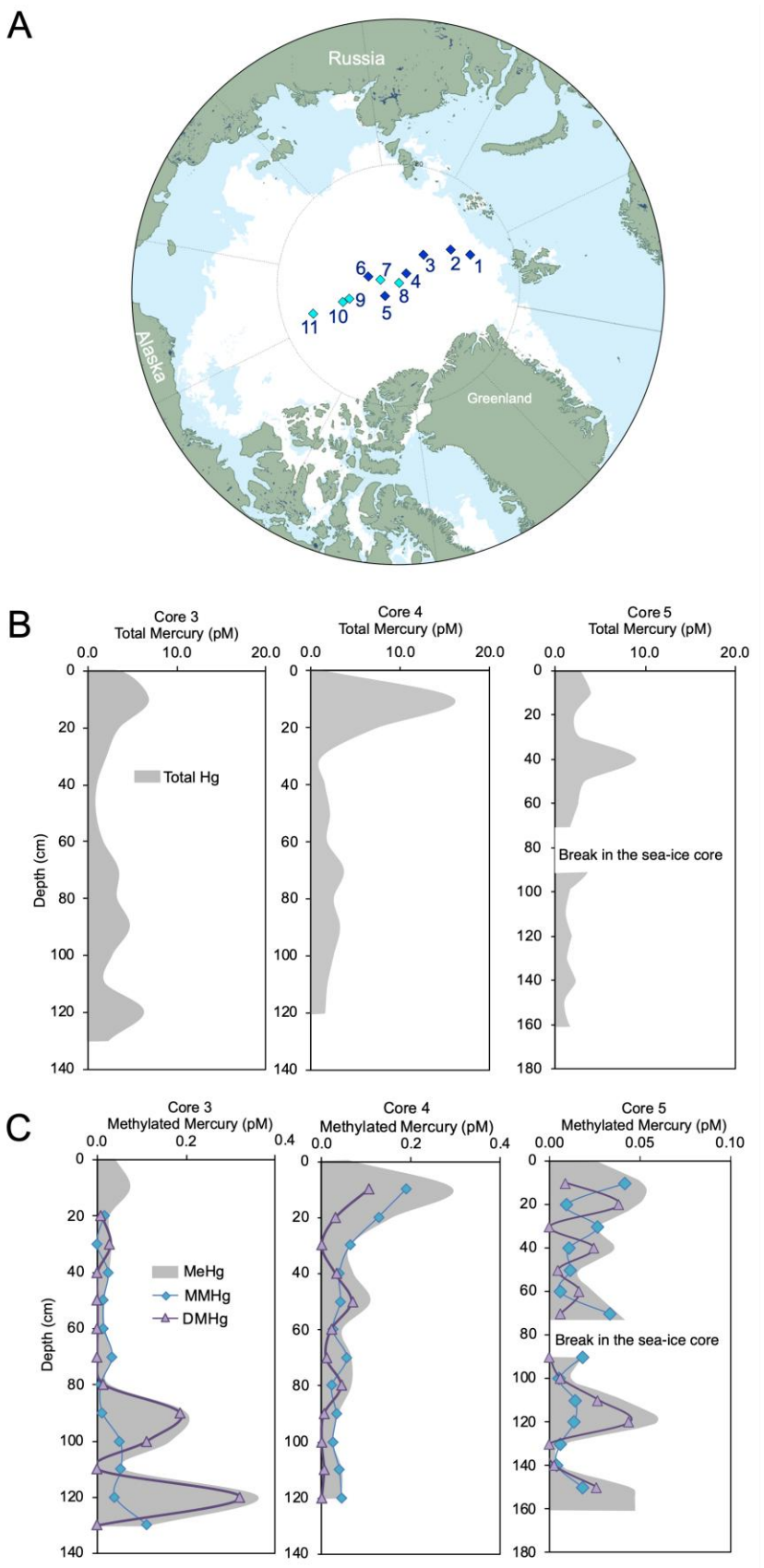
A
Russia
Alaska
Greenland
1
2
3
4
5
6
7
8
9
10
11
B
Core 3
Total Mercury (pM)
Core 4
Total Mercury (pM)
Core 5
Total Mercury (pM)
Depth (cm)
Total Hg
Break in the sea-ice core
C
Core 3
Methylated Mercury (pM)
Core 4
Methylated Mercury (pM)
Core 5
Methylated Mercury (pM)
MeHg
MMHg
DMHg
Break in the sea-ice core

386 **Figure 1**

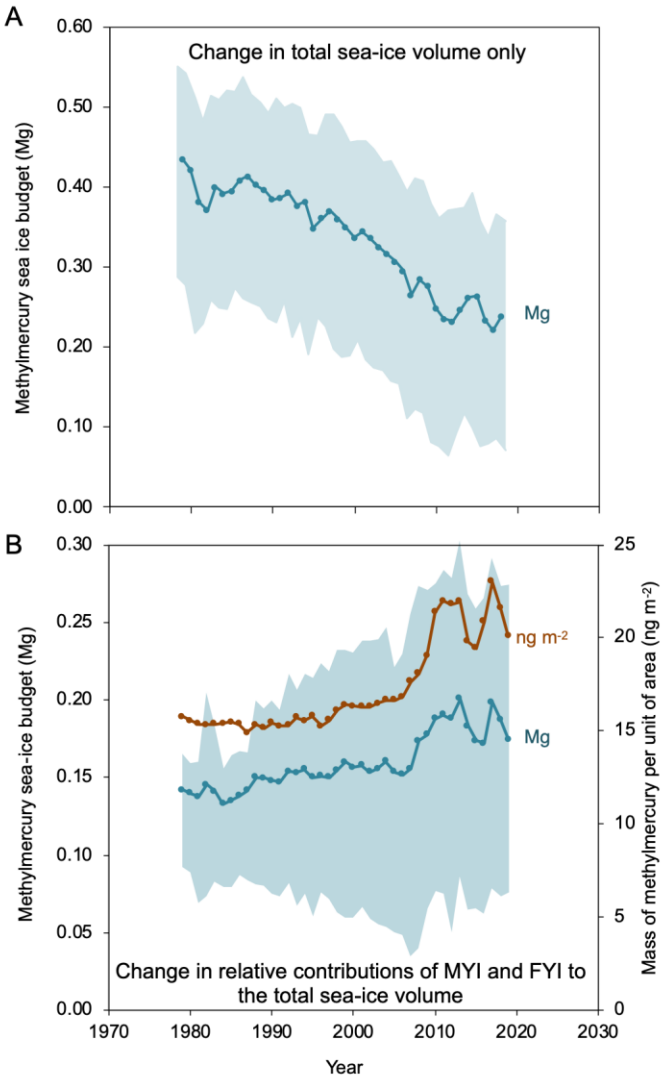
A
Change in total sea-ice volume only
Methylmercury sea ice budget (Mg)
0.60
0.50
0.40
0.30
0.20
0.10
0.00
Mg
B
Methylmercury sea-ice budget (Mg)
0.30
0.25
0.20
0.15
0.10
0.05
0.00
25
20
15
10
5
0
Mass of methylmercury per unit of area (ng m-2)
ng m-2
Mg
Change in relative contributions of MYI and FYI to the total sea-ice volume
1970
1980
1990
2000
2010
2020
2030
Year

Figure 2